Hindawi Publishing Corporation
Advances in Acoustics and Vibration
Volume 2012, Article ID 689379, 10 pages
doi:10.1155/2012/689379

Research Article

Microphone Arrays as a Leakage Detection Tool in Industrial Compressed Air Systems

Petr Eret and Craig Meskell

Department of Mechanical and Manufacturing Engineering, Trinity College Dublin, Parsons Building, Dublin 2, Ireland

Correspondence should be addressed to Petr Eret, petr.eret@tcd.ie

Received 27 April 2012; Revised 4 October 2012; Accepted 30 October 2012

Academic Editor: Arnaud Deraemaeker

Copyright © 2012 P. Eret and C. Meskell. This is an open access article distributed under the Creative Commons Attribution License, which permits unrestricted use, distribution, and reproduction in any medium, provided the original work is properly cited.

Compressed air energy is expensive, but common in industrial manufacturing plant. However, a significant part of the generated compressed air energy is lost due to leakage. Best practice requires ongoing leak detection and repair. Leak detection in the ultrasonic frequency range using handheld devices is possible only over short distances as associated high-frequency sound is rapidly attenuated by atmospheric absorption. Pressurized air escaping to ambience also generates frequencies below 20 kHz. In this paper beamforming—a well known method for generating noise maps—is tested as a tool for localization of compressed air leaks at larger distances in the audible frequency range. Advanced beamforming methods in both time domain (broadband) and frequency domain (narrowband) have been implemented in a variety of situations on a laboratory experimental rig with several open blows representing leakage in a noisy environment similar to a factory setting. Based on the results achieved it is concluded that the microphone array approach has the potential to be a robust leak identification tool. The experience gained here can also provide useful guidance to the practitioner.

1. Introduction

Compressed air is an expensive industrial utility [1]. Over a long time period the associated operating energy costs are undoubtedly a dominant part of the overall cost of a typical compressed air system [2]. Nonetheless, compressed air is central to many manufacturing processes. It is used as a source of energy in pneumatic actuators, control valves, and mainly in open blow applications such as fluidizing, conveying, drying, cooling, purging, sealing, and cleaning. The utilization of energy in the application side of compressed air system is poor in all situations (see, e.g., Eret et al. [3]). Moreover, there is energy rejection in the form of heat during compressed air generation and energy loss from leakage in the rest of the system. The first means loss of a huge amount of low grade energy which is possibly recoverable, but the latter represents irreversible loss of the high quality energy with work potential. For a particular situation, Eret et al. [3] have shown that leakage is one of the biggest consumers of the total generated compressed air. The leakage accounted almost for 21% and this result corresponds well with the best practice estimates (20–30%) [4].

Acoustic emissions, or simply acoustics, can play important role in understanding compressed air leakage. In the case of structure borne acoustic activity monitoring two examples related to compressed air are given. Augutis and Saunoris [5] investigated the internal leakage in a pneumatic cylinder using ultrasonic acoustics. They found that in the case of worn cylinder leakage between the piston and housing causes a higher intensity of acoustic emissions than in leak-free new cylinder. Prateepasen et al. [6] presented a portable noninvasive instrument for detection of the internal air leakage of a valve in a distribution system. Generally structure borne acoustic activity monitoring requires a good access to the potentially leaky spot. Moreover, there must be a space for installation of sensors on suitable materials

with low absorption as high-frequency components of the acoustic emission signal emitted from the leakage are investigated. Sometimes additional information is necessary; for example, knowledge of background interference from the plant must be determined by mounting the acoustic sensor to a part of the production line with no leakage. On the other hand, experience gained during compressed air system surveys showed that most leaks appear on small plastic tubing in loose connections, leaking proportional valves, or at inaccessible places. In situations like these, air borne acoustics is crucial in detecting compressed air leakage.

Compressed air leaking to ambient atmosphere creates broadband noise in both the audible and the ultrasonic frequency range. In industrial compressed air systems handheld ultrasonic sensors (usually operating around 40 kHz) are widely used tools for leakage localization. These instruments seem to be ineffective in noisy environments and must be operating at short distances, because high-frequency sound is rapidly attenuated by atmospheric absorption (see Wolstencroft and Neale [7]). As a result, a regular leak management programme is unattractive and missing on factory floors. The current study uses the concept of microphone array techniques operating in the audible frequency range (20 Hz–20 kHz approx.) as an alternative compressed air leakage detection tool. The associated data processing methods (beamforming) have been successfully applied in many aeroacoustic applications, where broadband noise sources are masked by larger ones and by external noise. The objective of this work is to show the applicability of microphone array techniques to compressed air leak detection using a simple experimental rig with several open blows representing leaks in noisy environment.

2. Basic Review of Beamforming Techniques

Beamforming has become a standard method for creating spatial noise maps. The sensor array techniques succeed in many applications such as aeroacoustics, geophysical processing, astronomy, and speech recognition. The concepts, working principles, and various techniques of microphone arrays are well described in the book by Johnson and Dudgeon [8]. The simplest algorithm of beamforming, corresponding to the basic "delay and sum" beamformer in the time domain, is shown schematically in Figure 1. The microphone array is virtually focused on each point of the measurement plane (or object in 3D) and the relative signal time delays between microphones are calculated. The signals recorded by the microphones are compensated for each focus point by the associated propagation delay, summed, and normalized by the number of microphones. Throughout this work, calculation of distances and delays will be used as shown in Figure 1, because it is equivalent to the spherical wave model of noise propagation and automatically tends towards a plane wave model for long distances. The well known issues associated with beamforming such as undesired effects of sidelobes, poor contrast of the noise maps, or weak sound sources masking have been gradually overcome by more advanced techniques, which will be used here for

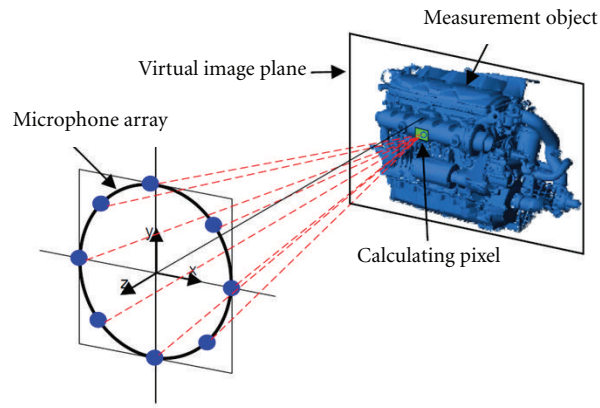

Figure 1: Principle of beamforming (picture reproduced from [9]).

compressed air leak detection. In principle, beamforming can be performed in two computational domains, time or frequency.

There are several benefits of beamforming in time domain. The main advantage of this approach is the ability to directly deal with short pulses, transients, and broadband signals. Broadband noise sources or a mixture of broadband noises are common in a manufacturing environment. Another practical important advantage of the time domain approach is the high computational efficiency due to the fact that computing time scales linearly with channel number. There is also a possible positive side effect of the explicit time domain broadband computations as there are less aliasing problems [10]. Finally, implementation of Doppler corrections for fast moving noise sources is easier in the time domain. This can be utilized when investigating airframe or jet noise in high-speed flights using phased microphone array. However, the benefits must be sometimes offset by higher sampling rates and processing of the huge amount of data. The drawbacks and benefits have been summarized by Jaeckel [10]. The simplicity of this approach was usually overlooked and only a few advanced techniques have been so far developed [11, 12]. These are discussed below and tested.

Frequency domain methods are mostly limited to processing narrow bands of frequencies and although several broadband approaches have been developed it is a common practice to apply these techniques to broadband signals over a representative frequency range. The basic way to process phase array data in the frequency domain is conventional beamforming. A crucial step is formation of the cross-spectral matrix (CSM). The beamforming process requires the CSM for each frequency. The beamformer output power gives a good estimation of a single source power. In a case of multiple sources, the quality of the estimation depends on the beamformer characteristics and therefore on the source locations, the frequency, and the number and distribution of the microphones in the array. The estimate of source location and power may be wrong especially for frequencies with wavelengths not small compared to the array aperture or for sources close to each other. This limits the usefulness of the

conventional beamformer [13]. In order to remove microphone self-noise the main diagonal of the cross-spectral matrix is deleted, because self-noise is not coherent between microphones and therefore does not contaminate the off-diagonal elements. This improves the contrast (dynamic range) of the noise maps. On the other hand, diagonal removal has an unpredictable influence on the absolute value of the beamformer [13]. Because implementation of advanced algorithms seems to be easier in the frequency domain, the literature offers many advanced beamforming techniques for improved mapping of acoustic sources such as deconvolution methods. DAMAS [14] by Brooks and Humphreys or CLEAN-SC [15] by Sijtsma, both being now standard tools in aeroacoustic measurements, are examples. The interested reader is referred to [15, 16] for more detailed review of the frequency domain beamforming techniques. For the purposes of this study, a robust deconvolution technique, superior to [14, 15] in terms of computational performance, proposed by Sarradj [13] is considered as well as conventional beamforming with diagonal deletion.

3. Applied Microphone Array Techniques

3.1. Time Domain. The calculation of noise maps in the time domain based on a "delay and sum" beamformer is the most intuitive method. Equation (1) expresses a general calculation of the beamformer b_{ds} at every location $\mathbf{x}$ (the potential source location) and time t, where m is the number of microphones, w_i is the optional spatial shading weighting factor (set to unity in all calculations here), p_i is the pressure time record of an individual microphone, and τ_i is the appropriate relative time delay. The beamformer output can be also normalized by number of microphones m, but this is omitted here for clarity. One has

$$b_{\mathrm{ds}}(\mathbf{x}, t) = \sum_{i=1}^{m} w_i p_i(t - \tau_i). \tag{1}$$

At each location $\mathbf{x}$ the source power of "delay and sum" beamformer is usually evaluated by the time average given in (2) assuming $w_i = 1$. One has

$$b(\mathbf{x}) = \frac{1}{T} \int_0^T \left[\sum_{i=1}^{m} p_i(t - \tau_i) \right]^2 \mathrm{d}t. \tag{2}$$

Dougherty [12] rewrote (2) as (3), where the first sum contains the autocorrelations of the microphone signals and the second sum contains the cross-correlations to be retained in the modified beamforming. By comparing (2) and (3) he presented modified "delay and sum" beamforming with diagonal deletion removing microphone self noise, which is defined by (4). The modification leads to improvement of the acoustic maps (increased dynamic range), but weak noise sources can still be masked by larger ones. One has

$$b(\mathbf{x}) = \frac{1}{T} \int_0^T \left[\sum_{i=1}^{m} p_i^2(t - \tau_i) + \sum_{i \neq k} p_i(t - \tau_i) p_k(t - \tau_k) \right] \mathrm{d}t, \tag{3}$$

$$b_{\mathrm{dd}}(\mathbf{x}) = \frac{1}{T} \int_0^T \left[\left[\sum_{i=1}^{m} p_i(t - \tau_i) \right]^2 - \sum_{i=1}^{m} p_i^2(t - \tau_i) \right] \mathrm{d}t. \tag{4}$$

Döbler and Schröder [11] introduced a simple technique to reveal weaker sources by subtractive signal decomposition. In this iterative process the reconstructed signal of the strongest source, which has the form of normalized equation (1), is sequentially translated by appropriate negative time delays and subtracted from all original microphone signals. This excludes the strongest signal from the noise map and further masked sources become visible. Although the technique cannot be applied to correlated sources, it suits well the separation of the broadband signals such as compressed air leaks, because they are uncorrelated signals as verified in Section 5.1 below.

3.2. Frequency Domain. The conventional beamforming in the frequency domain is basically defined by (5), where B is the beamformer output power, $\mathbf{G}$ (for the sake of simplicity the true cross-spectral matrix and its estimate due to the finite length of the measurement sample are not distinguished) represents the cross-spectral matrix ($m \times m$) of the microphone signals, and $\mathbf{h}$ is the steering vector ($h_i = e^{j\omega\tau_i}$). One has

$$B(\mathbf{x}) = \mathbf{h}(\mathbf{x})^{\mathrm{H}} \mathbf{G} \mathbf{h}(\mathbf{x}). \tag{5}$$

Sarradj [13] has used eigenvalue decomposition of the cross-spectral matrix $\mathbf{G}$ and proposed beamforming in the signal modal subspace, where individual eigenvalues and eigenvectors of the signal subspace are linked to the noise sources; the eigenvectors reveal the location of noise source while the eigenvalues contain information about the strength of the source. However, only the largest eigenvalues should be considered to get a number of potential sources. The technique is robust and fast in identification of multiple uncorrelated noise sources and offers a good spatial resolution in case of the weak noise sources. The essential mathematical tool is introduced below. Under the assumption that any sound source is uncorrelated to any additional noise signals, which are of equal amplitude n and also mutually uncorrelated, the cross-spectral matrix of the microphone signals $\mathbf{G}$ can be expressed by (6), where $\mathbf{A}$ represents matrix containing the transfer functions [13], $\mathbf{S}$ is the cross-spectral matrix of the source signals, and $\mathbf{I}$ is the identity matrix. One has

$$\mathbf{G} = \mathbf{A}\mathbf{S}\mathbf{A}^{\mathrm{H}} + n^2\mathbf{I}. \tag{6}$$

As the cross-spectral matrices are Hermitian and positive semidefinite, so the eigenvalue decomposition of $\mathbf{G}$ is

Table 1: Overview of beamforming methods used in tests.

Time domain (broadband)	Frequency domain (narrowband)
Diagonal deletion [12]	Diagonal deletion
Successive deletion of the main sources [11]	Orthogonal beamforming [13]

Table 2: List of test situations for beamforming.

Test 1: open blows near to each other at low pressure levels
Test 2: open blows at different positions
Test 3: effect of a dominant noise source behind the scan plane

possible. This leads to a diagonal matrix of eigenvalues $\mathbf{\Lambda}$ and a matrix of eigenvectors $\mathbf{V}$ as expressed in (7). The decomposition process can be further split into two parts according to the magnitude of eigenvalues as the smallest eigenvalues are considered to be all equal to n^2 and the cross-spectral matrix $\mathbf{G}$ can be explicitly viewed as a function of the source signals matrix of eigenvectors $\mathbf{V}_S$ and diagonal matrix of eigenvalues $\mathbf{\Lambda}_S$. One has

$$\mathbf{G} = \mathbf{V}\mathbf{\Lambda}\mathbf{V}^{\mathrm{H}} = \mathbf{V}_S\mathbf{\Lambda}_S\mathbf{V}_S^{\mathrm{H}} + n^2\mathbf{I}. \tag{7}$$

From each eigenvalue λ_{Si} and the appropriate eigenvector $\mathbf{v}_i$ a component of the decomposed cross-spectral matrix $\mathbf{G}_i$ can be calculated as follows:

$$\mathbf{G}_i = \mathbf{v}_i\lambda_{Si}\mathbf{v}_i^{\mathrm{H}}. \tag{8}$$

Equation (9) expresses the modified beamforming in subspaces based on decomposed cross-spectral matrices to create map for each eigenvalue, where $\mathbf{h}$ represents the standard definition of steering vector for the location $\mathbf{x}$ [13]. The map is the output of the spatial beamforming filter for only one single signal source which means that the highest peak in the map is the estimate of the signal source location. One has

$$B_i(\mathbf{x}) = \mathbf{h}(\mathbf{x})^{\mathrm{H}}\mathbf{G}_i\mathbf{h}(\mathbf{x}). \tag{9}$$

3.3. Summary of Applied Beamforming Methods. Table 1 summarizes beamforming techniques in both time and frequency domains tested for compressed air leak detection. The intention of the work is to compare the behavior of two different approaches, that is, time domain (broadband) and frequency domain (narrowband) beamforming in the same tests of various situations. For the sake of clarity these test cases are listed in Table 2 and detailed later. The most salient results are described in Section 5.2.

4. Experimental Setup

4.1. Two Open Blows Testing. A simple experiment has been carried out in order to assess the correlation of two identical open blows of 4 mm diameter at same pressure level as uncorrelated noise signals are easier to identify using all advanced beamforming techniques. Figure 2 illustrates a simplified schematic of the test of the two open blows located half a meter away from each other. The microphones are placed 10 cm away from the open blow axis to avoid turbulence effects on signal reception. The signal records of 10 seconds have been simultaneously sampled at 40 kHz to cover full audible range (20 Hz–20 kHz). The standard magnitude squared coherence between two signals is calculated by Welch's averaged, modified periodogram using a periodic Hamming window method with 50% overlap for 100 consecutive blocks each with 4096 samples. This high number of samples in the window is used for correlation tests only.

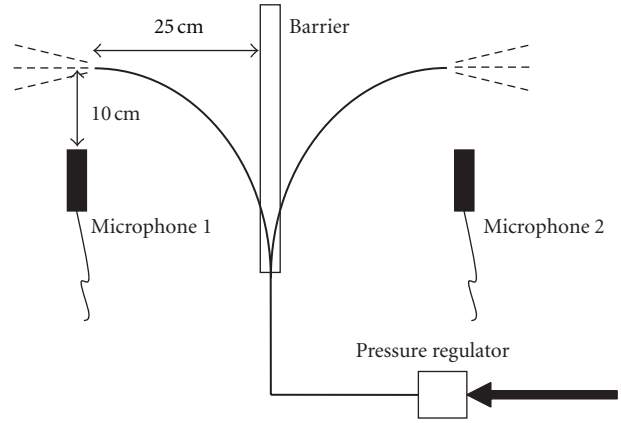

Figure 2: A schematic of two open blows test.

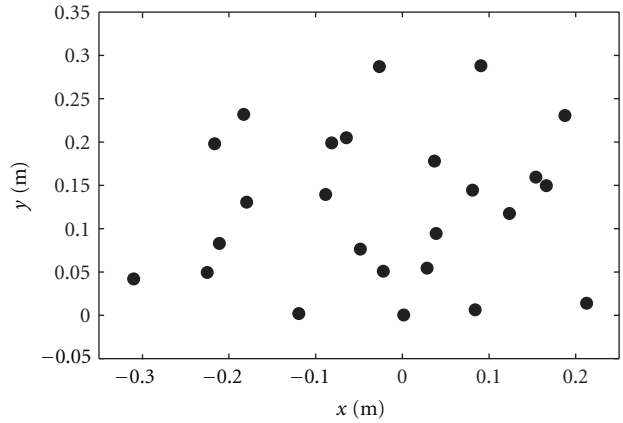

Figure 3: Front view of microphone array pattern.

4.2. Microphone Array for Compressed Air Leak Detection. A new microphone planar array with a small camera has been built for the core of the experimental work. An irregular pattern of 25 microphones has been used to avoid spatial aliasing typical of a regular array. Figure 3 shows the front view of the positions of the microphone over relatively small aperture designed for practical reasons. The signals from the Senheiser electret microphones with 20 Hz–20 kHz band pass filters are amplified before being simultaneously sampled using a National Instrument data

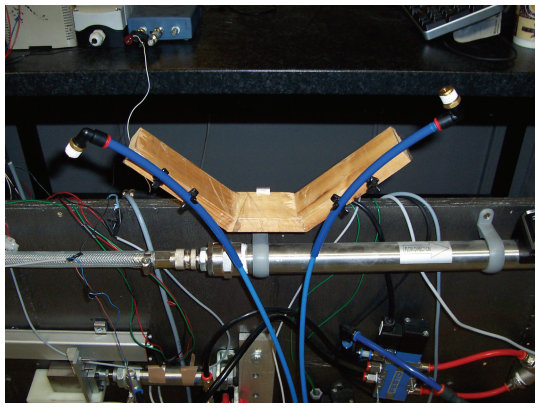

Figure 4: Typical configuration of open blows.

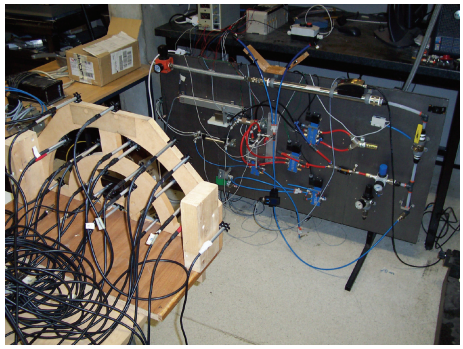

Figure 5: Experimental setup.

acquisition system. The instrumentation is similar to that used by Garcia-Pedroche and Bennett [17]. The data is processed using Matlab. The leaks are represented by small open tube blows connected to an already existing panel with several pneumatic components. Figure 4 details open blows in one of the situations under test. The compressed air is supplied at a pressure of 9 bar(a) approximately and reduced down to desired levels using a pressure regulator. Figure 5 depicts the position of the microphone array and the pneumatic panel under investigation, which is 1 m away from the sensors. The whole experimental setup is located in the reverberant environment with running machines in the background, so measurement conditions are similar to those of industry. The beamforming tests were carried out over a scan plane of 0.4 m $\times$ 0.4 m with step resolution of 0.01 m. Following the experience of Jaeckel [10] the sampling rate for the time domain beamforming was set high. Although it is recommended to use a sampling rate of 192 kHz to cover the audible frequency range, our system can operate only up to 100 kHz. The necessity of high sampling rate was compensated by a small amount of data (1000 points) to provide fast calculations (in the order of seconds). The raw time signals have been high-pass-filtered (frequencies up to 2 kHz removed) to reduce the effect of the background (running ventilators). However, there is space for improvement of the time domain technique as only half of the suggested frequency rate is used; this would lead of course to finer noise maps. The sampling rate for frequency domain beamforming was set to 40 kHz and time duration of the data acquisition was 0.5 seconds. The raw time data was band pass filtered (1 kHz) with a central band frequency of 15.5 kHz, because beamforming at higher frequencies provides a more accurate estimation of noise source location. Different window sizes of 1024 and 2048 samples with 50% overlap have been tested with no major difference in the final results.

5. Results

5.1. Two Open Blows Testing. Figure 6 shows the averaged coherence spectra for selected system pressure levels with a frequency resolution of 10 Hz. The background noise at zero gauge pressure captured by microphones is causing several high coherence intervals along frequency axis due to running of the machines (with distinctive tonal sounds) in the test room, which can be seen from Figure 6(a). With increasing pressure the open blow noise dominates over background noise and the true character of the flow induced noise can be revealed, because coherence tends to be more flat (Figure 6(b)). The constant low coherence at higher pressure levels (Figure 6(c)) indicates that the same compressed air open blows do not correlate in full frequency range. This fact can be also intuitively translated to compressed air leaks appearing at different pressure levels as will be clear from microphone array measurements mentioned later. The behavior is summarized in Figure 7, where mean coherence over the investigated frequency range for each tested pressure level is shown. The result means that compressed air open blows representing leaks are satisfactorily uncorrelated noise sources by nature and hence advanced beamforming techniques can be well utilized to separate them.

5.2. Microphone Array for Compressed Air Leak Detection. Test 1: *Open Blows Near to Each Other at Low Pressure Levels.* Two closely located (6 cm vertical separation) open blows with small volumetric flow rates (10 and 12 Nl/min) have been tested. The flow rates have been measured by Festo SFAB and Testo 6442 flow meters. The static pressure of 1.05 bar(a) was measured before the tube bifurcation using a small SMC pressure transducer; the pressure level at the main pressure regulator is slightly higher due to the pressure drop. The open blows were blowing in the opposite directions with the lower open blow downwards approximately 30 degrees off the vertical axis. For a human observer standing beside the microphone array these leaks were undetectable due to the overwhelming background noise. Nonetheless output from beamforming was satisfactory. Figure 8 shows time domain beamforming with diagonal deletion. In each plot the highest displayed level is normalized to 0 dB. The positions of the open blows are indicated by white circles in all figures. Similarly, the output from conventional beamforming in frequency domain with removal of microphone self noise is shown in Figure 9. It is apparent that time domain method gives better noise map than frequency domain beamformer.

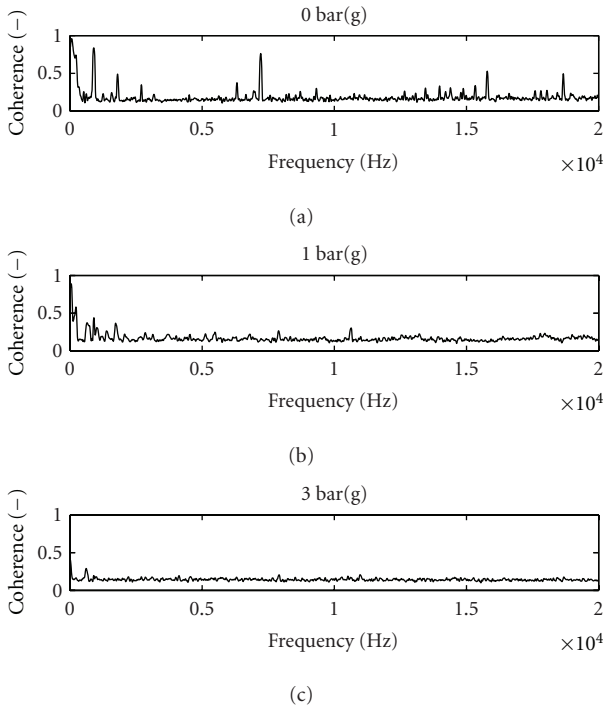

Figure 6: Coherence at various pressure levels.

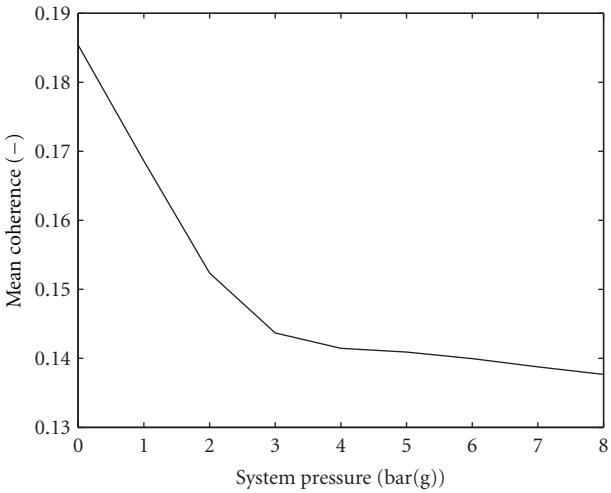

Figure 7: Mean coherence over audible frequency range at various pressure levels.

However, signal decomposition failed in both cases even when one source has been relocated (see Test 2). At slightly higher pressure level of 1.1 bar(a) and flow rates of 15 and 18 Nl/min, orthogonal beamforming starts to perform well in terms of the signal decomposition (spatial resolution) and surpasses considerably time domain technique. Figures 10 and 11 show the first and second mode, respectively. The peaks in the noise maps match well with the positions of the open blows.

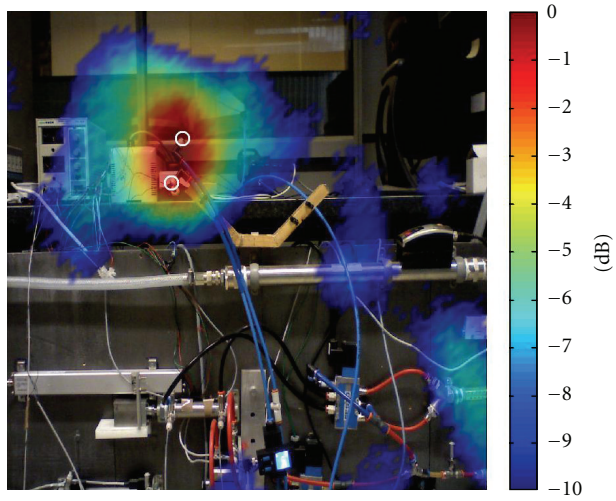

Figure 8: Time domain beamforming with diagonal deletion (2–20 kHz): two close open blows at low pressure level.

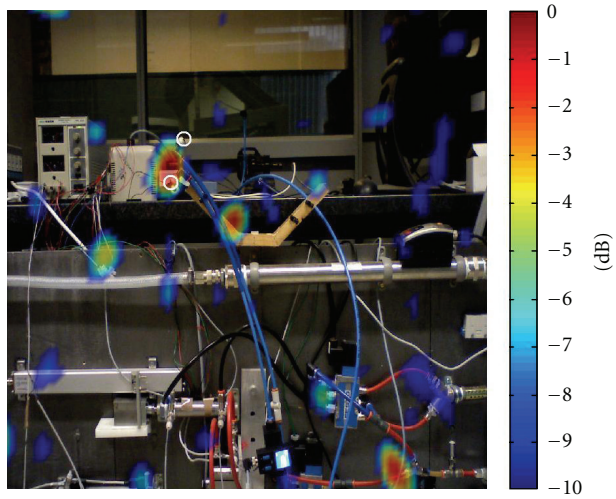

Figure 9: Frequency domain beamforming with diagonal deletion @15.5 kHz: two close open blows at low pressure level.

At this point it should be noted, that the estimation of the leakage position is the priority rather than quantifying generated sound pressure level and associated leakage flow rate. Experience revealed that open blow with relatively small flow rate can generate more noise at the same pressure level than a bigger one depending on the direction of the flow, inner geometry of the end piece, and open blow surroundings. This means that any effort to produce calibrated noise maps with respect to leak flow rate is impractical.

Test 2: Open Blows at Different Positions. Figure 12 shows noise map calculated from time domain beamforming for two spatially distinct (35 cm apart) open blows at a pressure of 1.3 bar(a). Now the signal subtraction is also possible in the time domain as shown in Figure 13. The minor source is dominant after the first iteration of the successive main

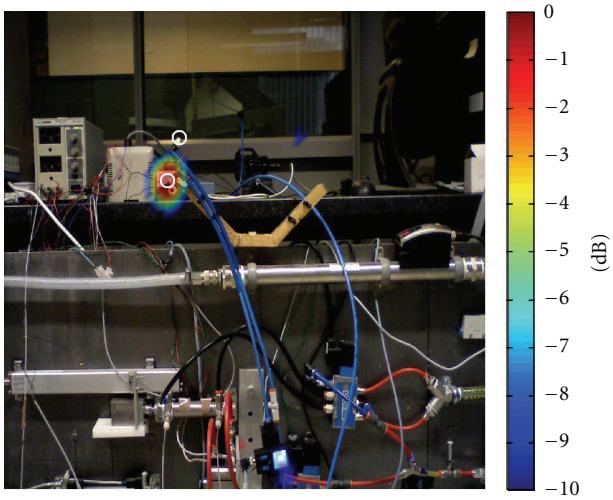

Figure 10: Orthogonal beamforming @15.5 kHz: two close open blows at low pressure level, first mode.

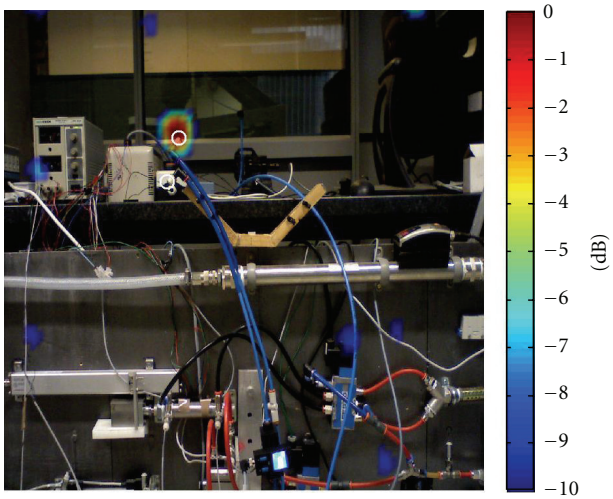

Figure 11: Orthogonal beamforming @15.5 kHz: two close open blows at low pressure level, second mode.

source deletion; however, a low dynamic range of the noise map is available. In general signal decomposition performs more effectively in the frequency domain approach due to the very robust eigenvalue decomposition. Figure 14 depicts the same situation based on conventional beamforming and reveals the drawback of the narrow band beamforming. The power intensities of the two sources are reversed, which would suggest that weaker source is generating more energy in the frequency range under investigation than the stronger one. When a different frequency band pass is chosen for beamforming, then the noise map corresponds to the result from the time domain. Nevertheless, estimations of noise source position are accurate in both cases, which is of importance.

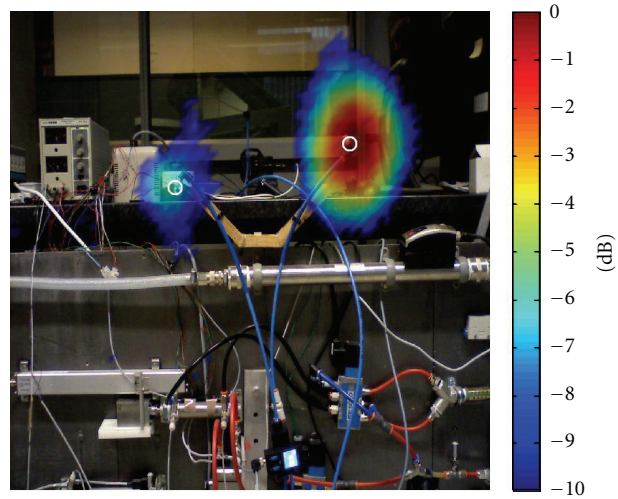

Figure 12: Time domain beamforming with diagonal deletion (2–20 kHz): two open blows at higher pressure level.

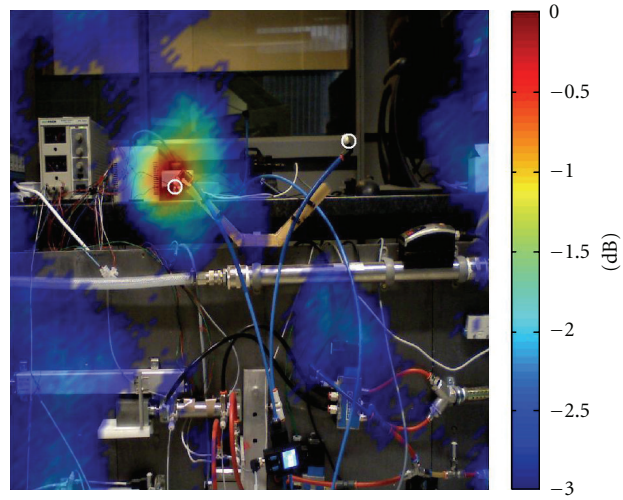

Figure 13: Time domain beamforming (2–20 kHz): after successive deletion of the main source on the right.

Test 3: *Effect of a Dominant Noise Source behind the Scan Plane.* A situation with two open blows located in the scan plane (open blow on right is throttled) and a far away dominant source was investigated at a measured pressure of 1.57 bar(a). A dominant open blow was placed 2 meters away from the microphone array (i.e., one meter behind the scan plane) close to the glass wall. The open blow was directed towards the wall at an angle of 30 degrees to excite reflections. For a human observer standing beside microphone array only this dominant source was obvious. Figure 15 shows result from time domain beamforming with diagonal deletion. The locations of all three sources are clearly visible and no significant reflections on the glass wall can be seen. This can be attributed to the broadband character of the open blow as energy is dispersed in the large space. Figure 16 shows a noise map based on conventional beamforming with

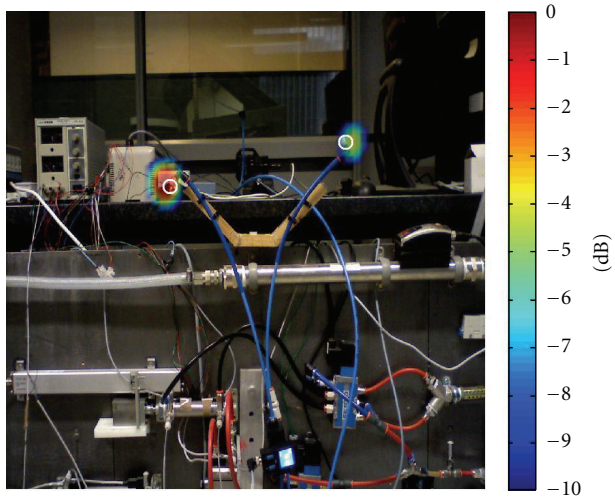

Figure 14: Frequency domain beamforming with diagonal deletion @15.5 kHz: two open blows at higher pressure level.

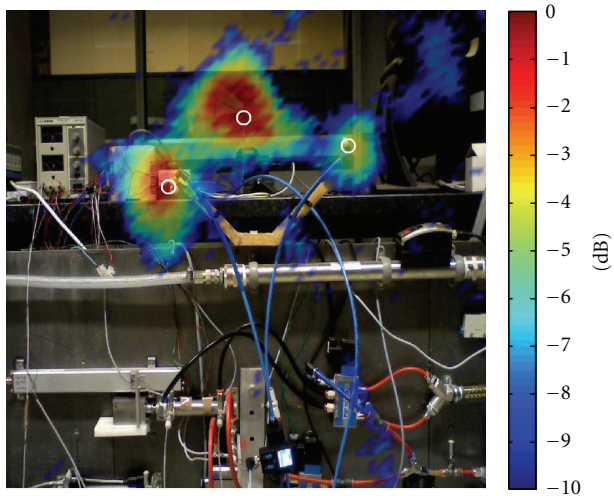

Figure 15: Time domain beamforming with diagonal deletion (2–20 kHz): two open blows with dominant source in the behind.

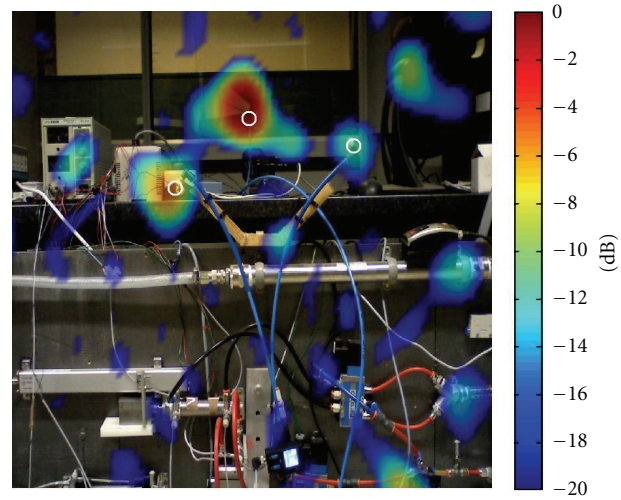

Figure 16: Frequency domain beamforming with diagonal deletion @15.5 kHz: two open blows with dominant source in the behind.

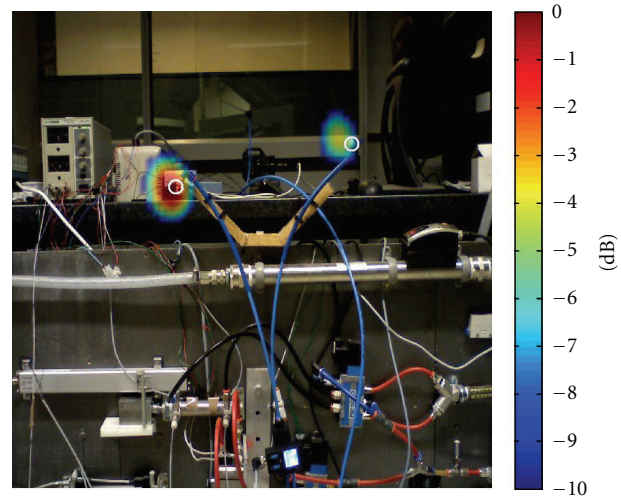

Figure 17: Orthogonal beamforming @15.5 kHz: two open blows with dominant source in the behind, second mode.

diagonal deletion. Despite the better contrast of the map, ghost images are present and locations of the minor sources are unclear as they are masked. The application of orthogonal beamforming offers a better picture on the leak locations. Figures 17 and 18 show positions of the peaks of the second and third mode, which correspond with the locations of the open blows.

6. Conclusions

Microphone array techniques operating in the audible frequency range have been used as a compressed air leak detection tool. The technique has been demonstrated on a laboratory experimental rig with several open blows representing leakage. Advanced beamforming methods in both time and frequency domains have been implemented in a variety of situations to test the performance of broadband (time domain) and narrowband (frequency domain) approaches. The time domain beamformer with diagonal deletion seems to perform better than the frequency domain conventional beamformer with diagonal deletion for generation of initial noise maps especially in a noisy environment, due to the fact that the broadband nature of the leakage is exploited. The narrowband frequency domain orthogonal beamforming is more effective in signal decomposition and spatial resolution. However, performance of the time domain beamformer tested here might be improved by higher sampling rates. The preliminary results have shown the applicability of the concept and suggest that the microphone array approach has the potential to be a robust leak identification tool in industrial settings.

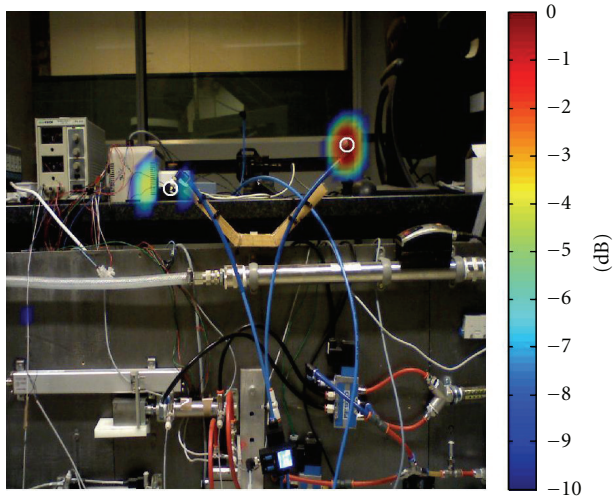

Figure 18: Orthogonal beamforming @15.5 kHz: two open blows with dominant source in the behind, third mode.

Nomenclature

$\mathbf{\Lambda}$: Diagonal matrix of eigenvalues of the microphone signals
$\mathbf{\Lambda}_S$: Diagonal matrix of eigenvalues of the source signals
λ_S: Eigenvalue of the source signal
ω: Frequency in rad/s
τ: Relative time delay
$\mathbf{A}$: Transfer functions matrix
$\mathbf{G}$: Cross-spectral matrix of the microphone signals
$\mathbf{h}$: Steering vector
$\mathbf{I}$: Identity matrix
$\mathbf{S}$: Cross-spectral matrix of the source signals
$\mathbf{V}$: Matrix of eigenvectors of the microphone signals
$\mathbf{v}$: Eigenvector of the microphone signal
$\mathbf{V}_S$: Matrix of eigenvectors of the source signals
$\mathbf{x}$: Location of the calculating pixel on noise map
B: Conventional beamformer output power in frequency domain
b: Beamformer output power in time domain
B_i : Subspace beamformer in frequency domain
b_{dd}: Beamformer output power with diagonal deletion in time domain
b_{ds}: Delay and sum beamformer in time domain
i: Index
j: Imaginary unit
k: Index
m: Number of microphones
n: Amplitude of noise
p: Pressure
T: Integration period
t: Time
w: Optional spatial shading weighting factor.

Acknowledgments

The research is cofunded by IRCSET and Intel. The authors are grateful for financial support.

References

[1] C. Y. Yuan, T. Zhang, A. Rangarajan, D. Dornfeld, B. Ziemba, and R. Whitbeck, "A decision-based analysis of compressed air usage patterns in automotive manufacturing," *Journal of Manufacturing Systems*, vol. 25, no. 4, pp. 293–300, 2006.

[2] Carbon Trust, "GPG 241—Energy Savings in the Selection, Control and Maintenance of Air Compressors," Tech. Rep., Carbon Trust, 1998.

[3] P. Eret, C. Harris, G. O'Donnell, and C. Meskell, "A practical approach to investigating energy consumption of industrial compressed air system. Proceedings of the Institution of Mechanical Engineers, Part A," *Journal of Power and Energy*, vol. 226, no. 1, pp. 28–36, 2012.

[4] SEI, Compressed air technical guide. Energy agreements programme—special working group on compressed air, Sustainable Energy Ireland, 2007.

[5] V. Augutis and M. Saunoris, "Investigation into acoustic emission of pneumatic cylinders," *Insight*, vol. 49, no. 8, pp. 476–480, 2007.

[6] A. Prateepasen, W. Kaewwaewnoi, and P. Kaewtrakulpong, "Smart portable noninvasive instrument for detection of internal air leakage of a valve using acoustic emission signals," *Measurement*, vol. 44, no. 2, pp. 378–384, 2011.

[7] H. Wolstencroft and J. Neale, "Characterisation of compressed air leaks using airborne ultrasound," in *Proceedings of Acoustics (AAS '08)*, Geelong, Australia, November 2008.

[8] D. H. Johnson and D. E. Dudgeon, *Array Signal Processing, Concepts and Techniques*, P T R Prentice Hall, Englewood Cliffs, NJ, USA, 1993.

[9] A. Meyer and D. D. Döbler, "Noise source localization within car interior using 3Dmicrophone arrays. BeBeC-2006-17," in *Proceedings on CD of the 1st Berlin Beamforming Conference*, November, 2006.

[10] O. Jaeckel, "Strengths and weaknesses of calculating beamforming in the time domain. BeBeC-2006-02," in *Proceedings on CD of the 1st Berlin Beamforming Conference*, November, 2006.

[11] D. Döbler and R. Schröder, "Contrast improvement of acoustic maps by successive deletion of the main sources. BeBeC-2010-19," in *Proceedings on CD of the 3rd Berlin Beamforming Conference*, February 2010.

[12] R. P. Dougherty, "Advanced time-domain beamforming techniques," in *Proceedings of the 10th AIAA/CEAS Aeroacoustics Conference*, pp. 1754–1764, Manchester, UK, May 2004.

[13] E. Sarradj, "A fast signal subspace approach for the determination of absolute levels from phased microphone array measurements," *Journal of Sound and Vibration*, vol. 329, no. 9, pp. 1553–1569, 2010.

[14] T. F. Brooks and W. M. Humphreys, "A deconvolution approach for the mapping of acoustic sources (DAMAS) determined from phased microphone arrays," *Journal of Sound and Vibration*, vol. 294, no. 4, pp. 856–879, 2006.

[15] P. Sijtsma, "CLEAN based on spatial source coherence," *International Journal of Aeroacoustics*, vol. 6, pp. 357–374.

[16] K. Ehrenfried and L. Koop, "Comparison of iterative deconvolution algorithms for the mapping of acoustic sources," *AIAA Journal*, vol. 45, no. 7, pp. 1584–1595, 2007.

[17] M. Garcia-Pedroche and G. J. Bennett, "Aeroacoustic noise source identification using irregularly sampled ldv measurements coupled with beamforming," in *Proceedings of the 17th AIAA/CEAS Aeroacoustics Conference (32nd AIAA Aeroacoustics Conference)*, Portland, Ore, USA, June 2011, (AIAA-2011-2719).

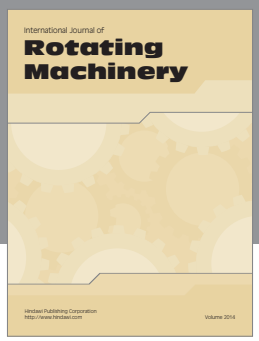

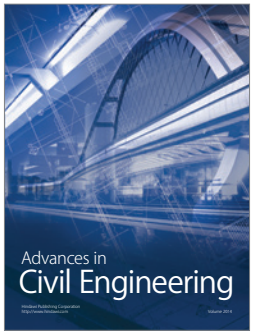

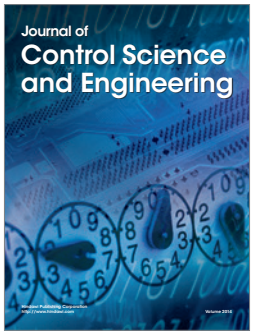

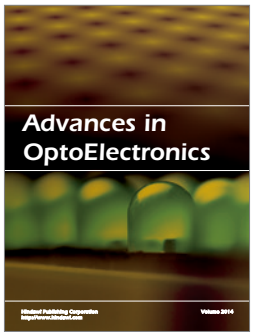

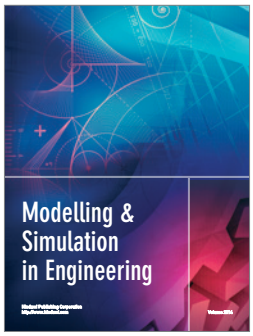

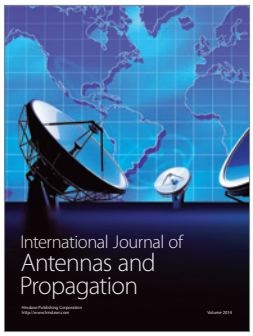

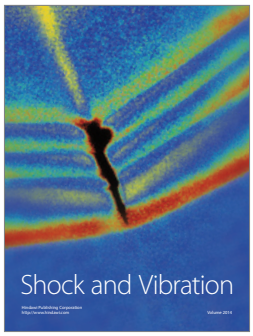

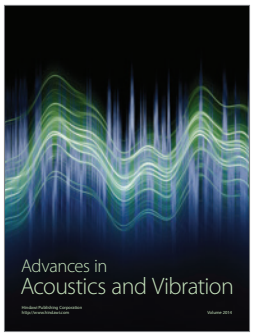

Hindawi

Submit your manuscripts at
http://www.hindawi.com